

APPLIED SCIENCES AND ENGINEERING

First analysis of ancient burned human skeletal remains probed by neutron and optical vibrational spectroscopy

G. Festa^{1*}, C. Andreani^{1,2,3}, M. Baldoni^{4,5}, V. Cipollari⁶, C. Martínez-Labarga^{3,4}, F. Martini⁷, O. Rickards^{3,4}, M. F. Rolfo⁸, L. Sarti⁹, N. Volante⁹, R. Senesi^{1,2,3}, F. R. Stasolla¹⁰, S. F. Parker¹¹, A. R. Vassalo¹², A. P. Mamede¹², L. A. E. Batista de Carvalho¹², M. P. M. Marques^{12,13}

Burned skeletal remains are abundant in archaeological and paleontological sites, the result of fire or of ancient funerary practices. In the burning process, the bone matrix suffers structural and dimensional changes that interfere with the reliability of available osteometric methods. Recent studies showed that these macroscopic changes are accompanied by microscopic variations are reflected in vibrational spectra. An innovative integrated approach to the study of archaeological combusted skeletal remains is reported here, where the application of complementary vibrational spectroscopic techniques—INS (inelastic neutron scattering), FTIR (Fourier transform infrared), and micro-Raman—enables access to the complete vibrational profile and constitutes the first application of neutron spectroscopy to ancient bones. Comparison with data from modern human bones that were subjected to controlled burning allowed identification of specific heating conditions. This pioneering study provides archaeologists and anthropologists with relevant information on past civilizations, including regarding funerary, burial, and cooking practices and environmental settings.

INTRODUCTION

Skeletal remains subject to burning events are often found in archaeological sites as a result of fire or ancient funerary practices and are usually the only preserved human vestiges. Following successful investigations on burned human bones by inelastic neutron scattering (INS) spectroscopy, aimed at relating burned to preburned parameters (1–6), the present study reports an innovative application of integrated vibrational spectroscopic techniques—Fourier transform infrared spectroscopy—attenuated total reflectance (FTIR-ATR), Raman, and INS—to extract information (i.e., cultural, biological, and environmental) from archaeological bones that were subject to heating. The correlation between the variations in the bone's chemical composition and crystallinity due to the burning process and the vibrational spectral profile will allow the interpretation of heat-induced changes in an accurate and quantitative way. Bone is a composite biomaterial mainly composed of packed collagen fibers and an inorganic matrix of crystalline hydroxyapatite (HAP) $[\text{Ca}_{10}(\text{PO}_4)_6\text{OH}_2]$, with the hydroxyl and phosphate groups partly substituted by carbonate (A- and B-type carbonates) (7–9). Bone mineral characteristics such as crystallinity or carbonate/phosphate content vary as a function of age, sex, location in the skeleton, diet, or

pathological state of the organism. With increasing temperature ($>200^\circ\text{C}$), the bone matrix suffers structural and dimensional variations, mostly related to microcrystallinity rearrangements usually leading to a higher crystallinity (10, 11). These are reflected in the vibrational response that can be detected by combined INS, FTIR, and micro-Raman techniques that have been recently applied by the authors to the investigation of burned human bones (1–6). INS, in particular, is an extremely well-suited technique for studying hydrogenous compounds. The neutron scattering cross section (σ) of an atom is characteristic of that atom and independent of the chemical environment. Because the value for hydrogen (80 barns) far exceeds that of all other atoms (typically ca. 5 barns), the modes with notable hydrogen displacement (u_i) dominate the spectra (12). Then, for a mode (i) at a given energy (v_i), the spectral intensity $[S_i(Q^2, v_i)]$ from a powdered sample obeys the simplified relationship

$$S_i(Q^2, v_i) = \frac{(Q^2 u_i^2) \sigma}{3} \exp\left(-\frac{Q^2 \alpha_i^2}{3}\right) \quad (1)$$

where Q (\AA^{-1}) is the momentum (wave vector, $k = 2\pi/\lambda$) transferred from the neutron to the sample and α_i (\AA) is related to a weighted sum of all the displacements of the atom. Hence, an INS experiment yields both the energies of the vibrational transitions (the eigenvalues, v_i) and the corresponding atomic displacements (the eigenvectors, u_i), adding to the information provided by the complementary Raman and infrared optical vibrational methods. High-quality INS spectra are measured for burned bones, as the features assigned to the bone's organic matrix are quite weak or even absent in samples subject to high temperatures. Hence, a clear detection of the signals from HAP is found, namely, the $\nu(\text{O-H})$ mode (ca. 3570 cm^{-1}) and the OH libration (ca. 630 cm^{-1}), which reveal the H-bond network within the inorganic lattice and are therefore highly sensitive to temperature changes (1, 4–6).

The use of INS spectroscopy to analyze the human bone is an innovative approach that is applied here to the study of burned archaeological skeletal remains. The specimens currently under study (both

¹CENTRO FERMI—Museo Storico della Fisica e Centro Studi e Ricerche “Enrico Fermi”, Piazza del Viminale 1, 00184 Rome, Italy. ²Università degli Studi di Roma “Tor Vergata”—Dipartimento di Fisica, Via della Ricerca Scientifica 1, 00133 Rome, Italy. ³Università degli Studi di Roma “Tor Vergata”—Centro NAST, Via della Ricerca Scientifica 1, 00133 Rome, Italy. ⁴Università degli Studi di Roma “Tor Vergata”—Dipartimento di Biologia, Via della Ricerca Scientifica 1, 00133 Rome, Italy. ⁵Università degli Studi di Roma “Tor Vergata”—Dipartimento di Biomedicina e Prevenzione, Via Montpellier 1, 00133 Rome, Italy. ⁶Soprintendenza Archeologica, Belle Arti e Paesaggio per l'area metropolitana di Roma, la provincia di Viterbo e l'Etruria meridionale, Via Cavalletti 2, 00186 Rome, Italy. ⁷Università degli Studi di Firenze—Dipartimento di Storia, Archeologia, Geografia, Arte e Spettacolo, Via S. Gallo 10, 50129 Florence, Italy. ⁸Università degli Studi di Roma “Tor Vergata”—Dipartimento di Storia, Patrimonio culturale, Formazione e Società, Via Columbia 1, 00133 Rome, Italy. ⁹Università di Siena—Dipartimento di Scienze Storiche dei Beni Culturali, Via Val di Montone 4—Via Roma 56, 53100 Siena, Italy. ¹⁰Sapienza Università di Roma—Dipartimento di Scienze dell'Antichità, Piazzale A. Moro 5, 00185 Rome, Italy. ¹¹ISIS Facility, STFC Rutherford Appleton Laboratory, Chilton, Didcot OX11 0QX, UK. ¹²University of Coimbra—Unidade de I&D “Química-Física Molecular”, Department of Chemistry, Coimbra 3004-535, Portugal. ¹³University of Coimbra—Department of Life Sciences, Coimbra 3000-456, Portugal.

*Corresponding author. Email: giulia.festa@centrofermi.it

human and faunal) were found in Italy at different archaeological sites from distinct periods—Neolithic, Copper Age, Roman, and the Middle Ages (Fig. 1 and table S1)—as follows:

1) The first set of human samples, from the Copper Age, was gathered in 2010 at the Scoglietto cave, a 40-m-deep cave located in the Parco Naturale Regionale della Maremma near Grosseto (Tuscany, Italy) (Fig. 1A) (13–15). On the basis of the available archaeological evidence, this cave is considered as one of the most significant Tuscan archaeological sites from between the Copper and Early Bronze Ages. A large structure for burning, in use and modified several times in antiquity, has survived in the back of the cave. This structure is referred to as Copper Age, and the radiocarbon dates place the structure for burning between 3360 and 2910 BCE (13–15).

2) The second group of ancient human skeletal remains is from the Middle Ages (500 to 1400 CE) and was found at the Leopoli-Cencelle archaeological site (Latium; Fig. 1B) (16–18). The bones currently analyzed were recovered during a 2014 excavation campaign in the church of St. Pietro (in the southeast area of the city) (16). Since 1532, Cencelle has been considered as a farm because of the presence of estates that specialized in supplying timber to the alum-based industries (16). The bones found at this site exhibited signs of combustion not related to funerary practices, which might have occurred at a later time.

3) A third group of human bones were collected at Guidonia-Montecelio (Latium) in the Le Pediche place (Fig. 1C). A necropolis dated from the Roman period (100 to 200 CE) was found at this site during excavations for construction of a road in 2014. One of the re-

covered individuals (from tomb 36) showed cremation features as bustum sepulcrum. The skeleton was found in anatomical connection, incorporated in a clay matrix, and placed supine with the arms along the pelvis. Inside the tomb, fragments of a lamp were also discovered, by the feet of the skeleton. It should be emphasized that such a lamp was found only in this bustum sepulcrum of the necropolis.

4) The fourth set of samples comprises one faunal bone found during the recent excavations at the Mora Cavorso cave (Neolithic archaeological site dated to 6000 to 5000 BCE; Fig. 1D), a multitunnel cavern with a complex stratigraphy located in southeastern Lazio (19). Its inner rooms revealed the presence of one of the most important funerary deposits from the Early Neolithic in central Italy. Around 30 individuals of all ages and both sexes (20), chaotically piled for natural and anthropic reasons, were found along with grave goods and ornaments. The macrofaunal assemblage consists of ca. 400 fragments, mostly attributed to domestic caprines and secondarily to cattle, dog, and red deer. This sample was investigated to verify the effectiveness of the applied spectroscopic methods to a faunal context.

Interpretation of the diagenetic alterations in the analyzed samples was based on vibrational spectroscopic results previously gathered for modern human bones burned under controlled temperatures (400° to 1000°C) (1, 3–6). A comparison between these data, taken as a reference, and that measured for the archaeological samples has led to an improved understanding of the changes elicited by the heating processes and of their effect on the bone's macroscopic characteristics (e.g., metric dimensions), yielding valuable information on ancient practices and customs.



Fig. 1. Archaeological sites where the samples investigated here were found. (A) Scoglietto cave: Hand distal phalanx and metacarpal bone. (B) Leopoli-Cencelle: Skull and tibia fragments. (C) Guidonia-Montecelio (tomb 36): Fibula, ulna, femur, and humerus fragments. (D) Mora Cavorso cave: Sheep/goat jaw fragment. Photo credits: G. Festa, Museo Storico della Fisica e Centro Studi e Ricerche “Enrico Fermi” (bones); F. Martini, Università degli Studi di Firenze (Scoglietto); F.R. Stasolla, Sapienza Università di Roma (Leopoli-Cencelle); V. Cipollari, Soprintendenza Archeologia del Lazio e dell’Etruria Meridionale (Guidonia-Montecelio); and M.F. Rolfo, Università degli Studi di Roma “Tor Vergata” (Mora Cavorso).

RESULTS

The combined use of the FTIR, Raman, and INS complementary techniques allowed access to the whole vibrational profile of the archaeological skeletal samples under study. FTIR-ATR and Raman yielded bands ascribed to phosphate [$\nu_2(\text{PO}_4^{3-})$, $\nu_4(\text{PO}_4^{3-})$, $\nu_1(\text{PO}_4^{3-})$, and $\nu_3(\text{PO}_4^{3-})$ at 470, 565, 603, and 960 cm^{-1} , respectively], carbonate [$\nu_2(\text{CO}_3^{2-})$ and $\nu_3(\text{CO}_3^{2-})$ at 870 to 880 cm^{-1} and 1415 to 1450 cm^{-1} , respectively], and protein (amide II and amide I at 1540 to 1580 cm^{-1} and 1665 cm^{-1} , respectively) (4, 5), as well as to chemical contaminants present in the remains. INS allowed an accurate detection of the features due to HAP's OH librational and stretching modes (at 630 and 3570 cm^{-1}), as well as of the characteristic low-frequency vibrations of the crystal lattice (below 500 cm^{-1}). The latter reflect variations in the short-range order and hydrogen-bonding profile within the bone's crystalline network and thus are being associated with the bone's dimensional changes. Special attention was paid to bands formerly identified as useful biomarkers of heat-prompted changes within the bone's crystalline framework (1, 5, 6): (i) HAP's OH libration, (ii) features due to $\nu_2(\text{PO}_4^{3-})$ and $\nu(\text{HPO}_4^{2-})$, and (iii) Ca^{2+} and PO_4^{3-} sublattice translational (ca. 320 to 190 cm^{-1}) and PO_4^{3-} librational (<190 cm^{-1}) modes. HAP's OH_{lib} , in particular, was found to be a very useful diagnostic signal of the burning process, as it was found to undergo a clear shift to lower energy with increasing burning temperature. Regarding INS, the use of three incident energies in the MAPS measurements (5240, 2024, and 968 cm^{-1}) enabled the simultaneous observation of all OH-related modes for the archaeological bones—libration and its overtones and stretching [which had only been achieved before for modern bone samples (1), using the same experimental procedure]. Moreover, combined measurements at MAPS and TOSCA spectrometers allowed access to the whole vibrational window of the samples from the low-frequency region to the high wave number range.

The spectroscopic data presently obtained for the ancient skeletal samples were interpreted in the light of the results formerly gathered for modern human bones burned (5) under controlled laboratory conditions (from 400° to 1000°C), currently taken as references: femur and humerus (osteometrically very informative). In accordance with these previous data, at temperatures below 400° to 500°C, the bones still retain part of their lipid and protein components [revealed by the $\delta(\text{CH}_2)_{\text{lipids}}$ and amide I_{protein} bands at 1450 and 1665 cm^{-1} , respectively], with these being completely destroyed above 500°C. For very high burning temperatures, in turn, the spectra reflected a progressive carbonate loss coupled with an increasing crystallinity of the inorganic matrix, resembling more and more the vibrational pattern of reference HAP. Figure 2 shows the FTIR-ATR and INS experimental data measured for human skeletal remains found at the Leopoli-Cencelle medieval archaeological site [fragments from tibia (US1241) and skull (US10143)], as well as a reference sample from modern bones. The infrared results evidenced that the medieval samples were subject to heating. Comparison with the infrared spectrum of an intact (modern) human bone showed no evidence of lipids [absence of the $\delta(\text{CH}_2)$ and $\nu(\text{CH})$ signals at 1340 to 1460 cm^{-1} and 2900 to 3000 cm^{-1} , respectively] and hardly any traces of protein, which would be evidenced by the amide I, amide II, and $\nu(\text{CH}_2)_{\text{collagen}}$ bands at 1570, 1665, and 2970 cm^{-1} , respectively (Fig. 2A). In addition, the presence of traces of fluorapatite [calcium fluorophosphate, $\text{Ca}_5(\text{PO}_4)_3\text{F}$, generally known as francolite] was revealed in these samples through the characteristic $\nu_3(\text{PO}_4^{3-})$ feature appearing as a shoulder at 1090 cm^{-1} on the very strong signal of the $\nu_1(\text{PO}_4^{3-})$ band (at 960 cm^{-1}).

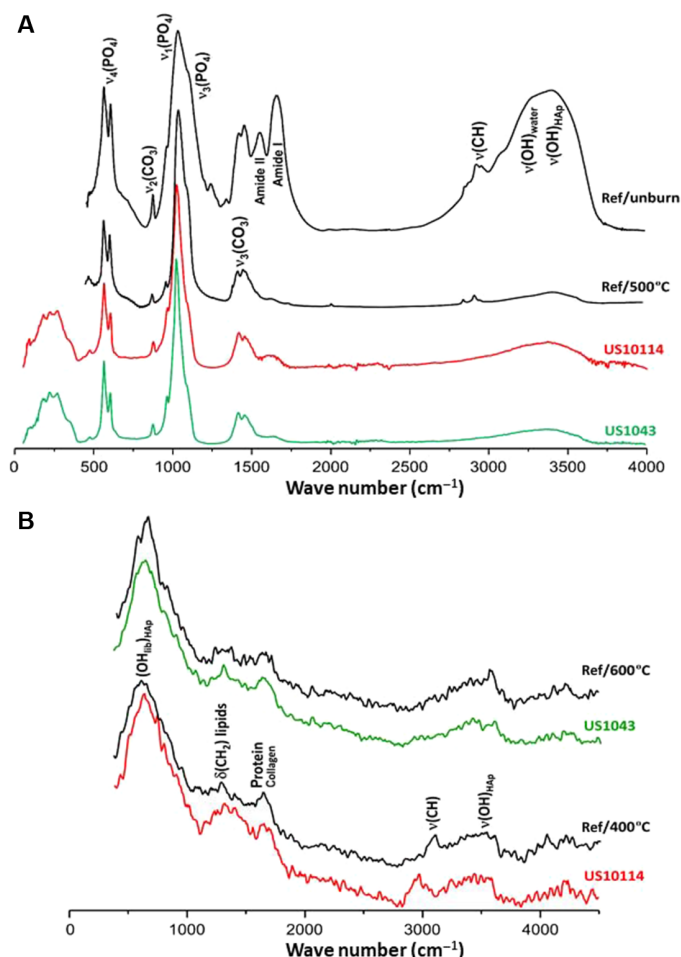


Fig. 2. Vibrational spectra of medieval human bones (Leopoli-Cencelle, Italy). Comparison with modern human bone samples (5) burned at 400°, 500°, and 600°C. (A) FTIR-ATR and (B) INS.

Regarding the INS results, a remarkable similarity was observed between the profiles of the modern and ancient samples (Fig. 2B). The presence of small amounts of lipids and proteins was shown, evidencing a higher sensitivity of the technique relative to FTIR for this kind of H-containing constituents. Furthermore, a reliable estimate of the temperature to which the archaeological samples were subject to was achieved: The vibrational profile of the skull fragment (US1043) was found to be comparable to the reference bone burned at 600°C, while that of the tibia (US10114) was identical to the 400°C reference. Notably, these two archaeological samples could only be discriminated through neutron techniques because the small chemical differences between them were not revealed by infrared spectroscopy. While the FTIR-ATR fingerprint (21, 22) of the medieval bones provided only an average temperature range to which the bones were exposed, INS yielded a precise burning temperature for each analyzed sample, being able to differentiate between 400°C (for the tibia) and 600°C (for the skull). Accordingly, these archaeological bones were probably subject to a char process (at 400° or 600°C), with a concomitant crystallinity increase and almost total loss of the organic constituents—the lipids having been completely destroyed above 400°C, while some collagen is still present within the bone matrix. In addition, the detection of francolite revealed the occurrence of fluoride

in the bone matrix, probably due to environmental contamination from either the neighboring soil or water.

The FTIR and INS spectra of human hand distal phalanx (PFF12) and metacarpal bone (PFF27) from the Copper Age, found at the Scoglietto cave, are shown in Fig. 3. The FTIR-ATR results show that these samples were subject to heating at temperatures not higher than 450° to 500°C. They display the typical infrared features of the bone still containing traces of protein (collagen I), mainly evidenced by the amide I band (Fig. 3A). The INS data go further in identifying some lipid components through the corresponding $\delta(\text{CH}_2)$ and $\nu(\text{CH})$ signals at ca. 1450 and 3000 cm^{-1} , respectively (Fig. 3B). Upon comparison with the data obtained for reference samples heated at defined temperatures, both spectroscopic signatures correspond to a burning temperature around 500°C, virtually homogeneous for the three ancient skeletal remains. This temperature is compatible with an incomplete cremation in home fires. Cremations are found in all

periods from the Neolithic to the Medieval Era and play an important role in ancient funerary practices (23).

Raman microspectroscopy measurements performed on these ancient samples provided clear evidence of the presence of gypsum (calcium sulfate dihydrate, $\text{CaSO}_4 \cdot 2\text{H}_2\text{O}$) through the distinguishing band from the sulfate symmetric stretching [$\nu_1(\text{SO}_4)$] at 1008 cm^{-1} and the $\nu_2(\text{SO}_4)$, $\nu_4(\text{SO}_4)$, and $\nu_3(\text{SO}_4)$ signals at 415/493, 670, and 1136 cm^{-1} , respectively (fig. S2) (24, 25). This constituent is indicative of contamination from the soil surrounding the skeletal remains, as this archaeological area is characterized by a cavernous limestone geology with a high gypsum content (26, 27).

Figure 4 displays the INS spectra of the human bones (one skeleton only) discovered in tomb 36 at the Guidonia-Montecelio Roman archaeological site. Different types of bones from this same skeleton displayed very different INS profiles, consistent with diverse heating conditions from below 400° up to 500° or 800° to 900°C. This can be

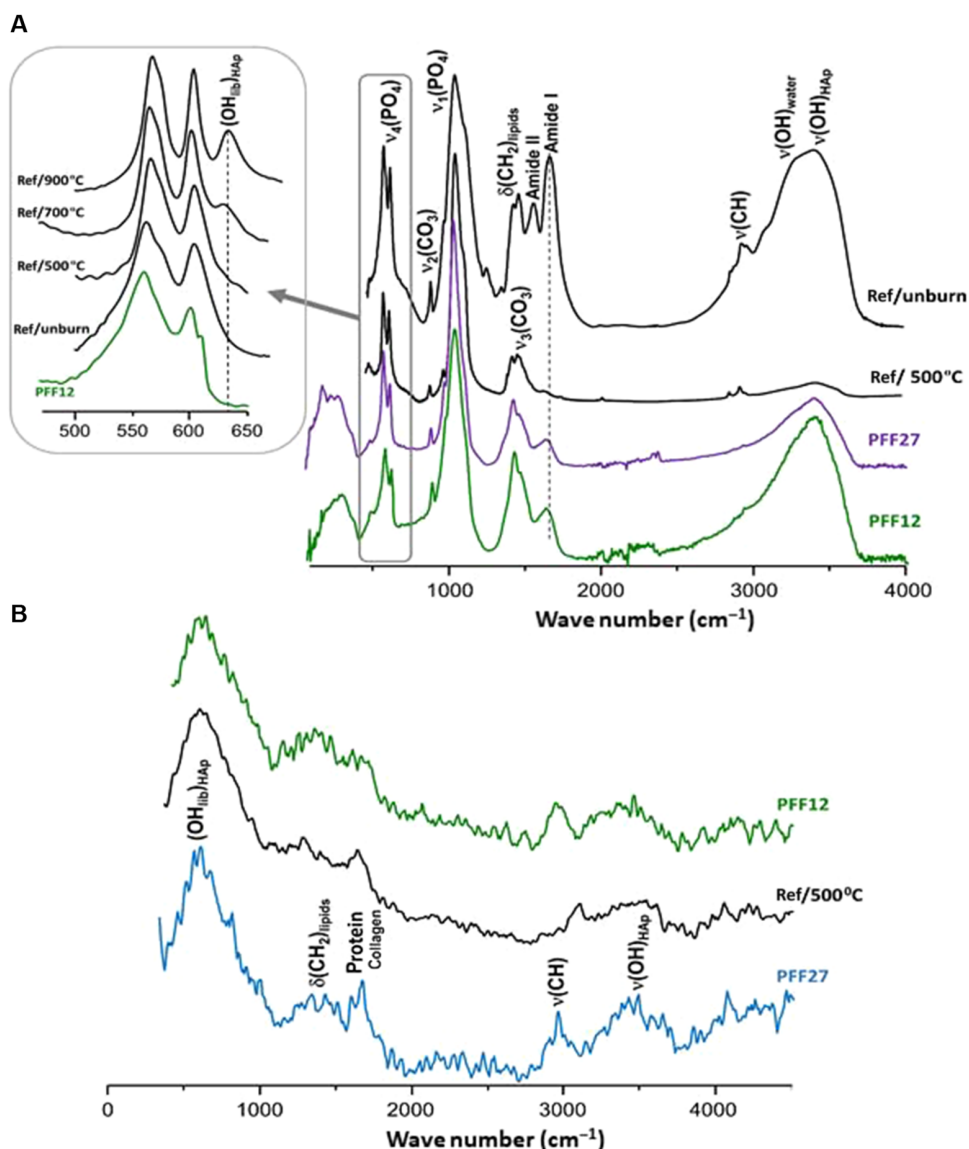


Fig. 3. Vibrational spectra of human bones from the Copper Age (Scoglietto cave, Italy). Comparison with modern human bone samples (5) burned at 500°C. (A) FTIR-ATR and (B) INS. The inset in (A) depicts the temperature dependence of the spectral profile in the interval of 500 to 650 cm^{-1} .

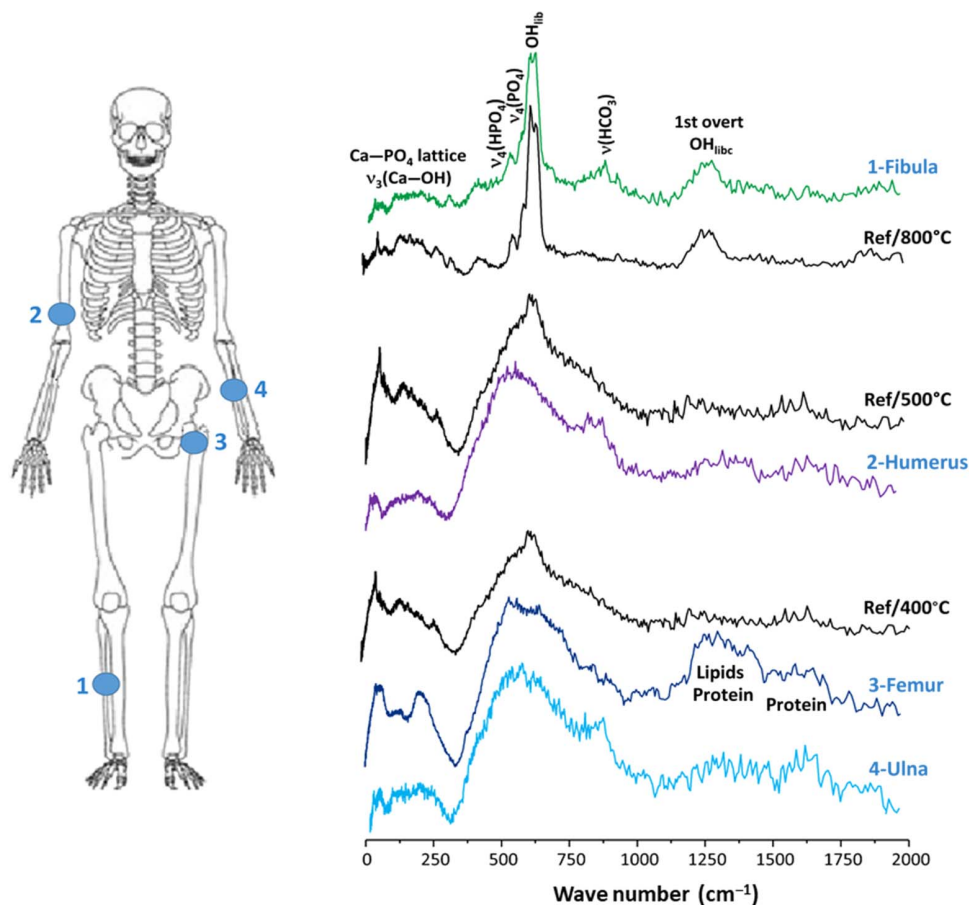


Fig. 4. INS spectra of different human bones from the Roman period [humerus, ulna, femur, and fibula from the same skeleton, Guidonia-Montecelio, Italy (tomb 36)]. Comparison with modern human bone samples (5) burned at 400°, 500°, and 800°C.

justified by ancient funerary practices that involved burning the bare corpses inside the grave. Moreover, relating the heating conditions with the type of bone—increasing temperatures for ulna, femur, humerus, and fibula—suggests that the body might have been folded in a fetal position. In addition, for some of these samples, a band at ca. 900 cm^{-1} , ascribed to $\nu(\text{HCO}_3^-)$, was detected (mainly for fibula), evidencing contamination from the soil that has a limestone composition in the Guidonia-Montecelio region (because the samples were found unwrapped inside the earth tomb). The major factors prone to influence the degree of combustion of the skeletal remains, and therefore the effect on bone composition and crystallinity, are the temperature, heating time, and environmental conditions (e.g., presence or absence of oxygen). The spectroscopic data depicted in Fig. 4 reveal that the lower area of the skeleton reached higher temperatures than the upper part. Coupled to the discovery of lamp fragments by the feet of the body, this can reveal the origin of the burning process. Moreover, it may evidence that the burning occurred in situ and that the lamp had an active role in this ritual funerary practice.

To assess the usefulness of the presently developed methodology and extend its capabilities beyond human skeletal remains, we also investigated the Neolithic faunal bones from the Mora Cavorso archaeological site. Figure 5 shows the FTIR-ATR spectra of a sheep/goat jaw fragment subject to heat, as compared to two modern human bones—unburned and burned at 500°C . By analysis of the most informative vibrational bands (from phosphate, carbonate, and the bone's organic compo-

nents), the archaeological remain appears to have been exposed to temperatures below 500°C , which is compatible with the temperatures reached in hearths used in ancient Neolithic settlements for cooking. However, care should be taken when interpreting these data because it was found that human and faunal bones display different reactions to heat, especially at higher temperatures (3).

DISCUSSION

An innovative approach to the study of burned archaeological bones is currently reported. Ancient skeletal remains (human and faunal) subject to burning events, found at several archaeological sites from the Neolithic, Copper Age, Roman, and Middle Ages, were investigated through complementary vibrational spectroscopic techniques. This integrated approach is here shown to allow an accurate and complete vibrational data to be obtained, which was previously inaccessible because of the almost exclusive application of infrared techniques, with Raman analysis being severely undermined by the very high fluorescence of the bone [when not subject to high temperatures ($>700^\circ\text{C}$)] even when using red excitation wavelengths (28). In addition, INS enables the observation of vibrational modes not detectable by optical techniques. The results obtained for the burned archaeological skeletal remains show a clear correspondence with the spectral trends formerly measured for modern human bones subject to different temperatures (1, 4, 5), providing relevant information on the original burning temperature, heating conditions, and

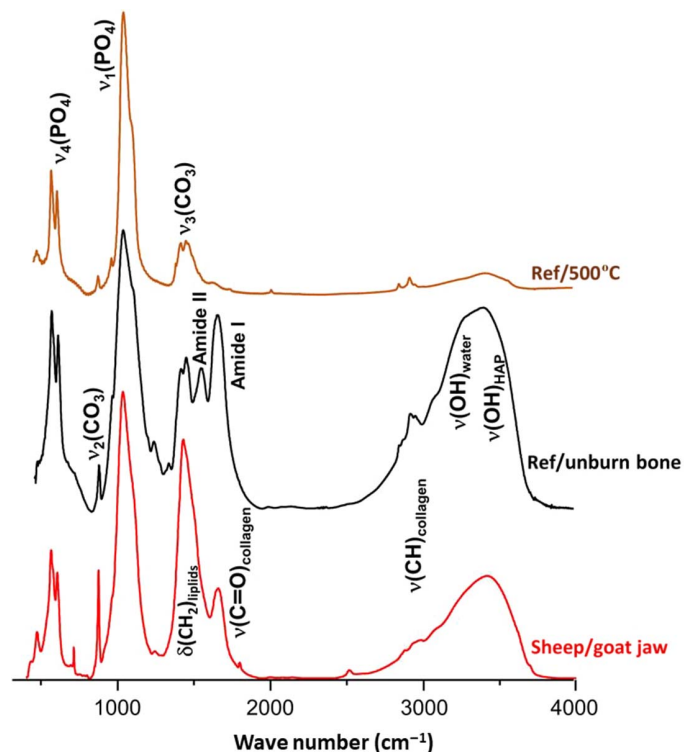


Fig. 5. FTIR-ATR spectra of Neolithic faunal bones (Mora Cavorso cave, Italy). Comparison with modern human bone samples (5), unburned and burned at 500°C.

environmental factors that affected the samples under study. The human bones coming from the Scoglietto cave displayed spectral signatures corresponding to burning temperatures lower than 500°C, well matched with incomplete cremation processes carried out in the home fires that were very common in the Copper Age. The medieval Leopoli-Cencelle samples, in turn, appeared to be burned in a nonuniform way for temperatures spanning from 400° to 600°C. As for the remains from the Guidonia-Montecelio Roman site, the data presently reported provided preliminary conclusions on the temperature to which they were exposed, as well as on the characteristics of the surrounding environment. Noticeably, they allowed us to identify a particular funerary practice that burned the bodies inside their graves, unwrapped, in direct contact with the soil. The results recorded for the sheep/goat jaw from Mora Cavorso, the only animal bone sample currently probed, were consistent with heating temperatures below 500°C, compatible with the Neolithic hearths probably used for cooking purposes.

This study constitutes the first application of neutron spectroscopy to archaeological skeletal remains and will allow archaeologists/anthropologists to gather relevant information on ancient civilizations regarding the locations and the funerary, burial, or cooking practices. Future research will enlarge the number of samples and archaeological sites to gather data on a wider range of contexts—geographical, historical, and anthropological. Further spectroscopic biomarkers will then be identified, enabling a precise statistical analysis of the results linking particular spectral signatures to specific burning scenarios and environmental settings.

MATERIALS AND METHODS

Archaeological skeletal remains (both human and faunal; Fig. 1) were analyzed (see details in table S1). All the archaeological samples under

study were measured as intact bone fragments after gentle mechanical removal of the outer layer to avoid contaminants. According to previous spectroscopic studies (1, 21, 22), no further cleaning was needed.

INS spectroscopy

INS measurements were performed at the ISIS Neutron and Muon Source of the Rutherford Appleton Laboratory (UK) using the high-resolution MAPS and TOSCA spectrometers (29, 30). The instruments are complementary, as explained elsewhere (30). For the present case, the key differences are that TOSCA provides high-resolution spectra for the range of 0 to 2000 cm^{-1} , while MAPS enables access to the C–H and O–H stretch regions. The bone samples were fixed onto (4 cm by 5 cm) flat Al cans with Al tape and wrapped in aluminum foil (fig. S1)—2 to 5 g for the intact archaeological bones and ca. 5 g for each reference sample, which was previously found to be an optimal amount (1–6). To reduce the impact of the Debye-Waller factor on the observed spectral intensity, the samples were cooled to cryogenic temperatures (ca. 5 to 10 K). Data on MAPS were recorded in the energy range of 0 to 5000 cm^{-1} using three incident energies (5240, 2024, and 968 cm^{-1}). For both instruments, the neutron data were reduced to energy transfer spectra using the MANTID software (version 3.4.0) (31). In addition, a spectrum of reference HAP was measured {highly crystalline, stoichiometric calcium hydroxyapatite, $[\text{Ca}_{10}(\text{PO}_4)_6(\text{OH})_2, \text{Ca}/\text{P} = 1.67]$, SRM 2910b, from NIST, Gaithersburg, MA, USA} (32).

FTIR spectroscopy

The FTIR-ATR spectra were measured at the Molecular Physical-Chemistry R&D Centre of the University of Coimbra [QFM-UC, Portugal (33)] using a Bruker Optics Vertex 70 spectrometer purged by CO_2 -free dry air. The mid-infrared absorbance spectra (between 400 and 4000 cm^{-1}) were recorded using a Ge on KBr substrate beam splitter and a liquid nitrogen-cooled wide band MCT (mercury cadmium telluride) detector. The far-infrared data (50 to 600 cm^{-1}) were obtained in a Bruker Platinum ATR single reflection diamond accessory using a silicon solid-state beam splitter and a DLaTGS (deuterated L-alanine-doped triglycine sulfate) detector with a polyethylene window. The spectra were corrected for the wavelength dependence of the penetration depth of the electric field in ATR using the standard Bruker OPUS software option. In both cases, spectra were the sum of 64 scans at a resolution of 2 cm^{-1} , and the three-term Blackman-Harris apodization function was applied. Under these conditions, the wave number accuracy was better than 1 cm^{-1} .

Raman spectroscopy

Raman microspectroscopy measurements were carried out at QFM-UC (Portugal) (33). The spectra were recorded in the range of 600 to 1800 cm^{-1} using a HORIBA Jobin-Yvon T64000 spectrometer in direct configuration mode (focal distance, 0.640 m; aperture, f/7.5), equipped with a holographic grating of 1800 grooves mm^{-1} . The entrance slit was set to 200 μm . Rayleigh elastic scattering was rejected by a notch filter, which reduces its intensity by a factor of 10^6 . The detection system was a liquid nitrogen-cooled non-intensified charge-coupled device camera [1024 × 256 pixels (1")]. The 514.5-nm line of an Ar^+ laser (model Innova 300-05, Coherent) was used as the excitation radiation, yielding ca. 10 mW at the sample position. All spectra were recorded using an Olympus 50× objective (MSPlan 50, infinity corrected; numerical aperture, 0.80; working distance, 0.47 mm). A 100- μm pinhole rejected signals from out-of-focus regions of the sample.

SUPPLEMENTARY MATERIALS

Supplementary material for this article is available at <http://advances.sciencemag.org/cgi/content/full/5/6/eaaw1292/DC1>

Supplementary Methods

Table S1. Archaeological human and faunal skeletal remains analyzed in the present study.

Fig. S1. An archaeological human skeletal remain placed onto an Al can and wrapped in Al foil, ready for INS measurement.

Fig. S2. Raman spectrum of a prehistoric human bone sample (Scoglietto cave, Italy), evidencing the presence of gypsum.

REFERENCES AND NOTES

- M. P. M. Marques, D. Gonçalves, A. I. C. Amarante, C. I. Makhoul, S. F. Parker, L. A. E. Batista de Carvalho, Osteometrics in burned human skeletal remains by neutron and optical vibrational spectroscopy. *RSC Adv.* **6**, 68638–68641 (2016).
- A. R. Vassalo, E. Cunha, L. A. E. Batista de Carvalho, D. Gonçalves, Rather yield than break: Assessing the influence of human bone collagen content on heat-induced warping through vibrational spectroscopy. *Int. J. Leg. Med.* **130**, 1647–1656 (2016).
- D. Gonçalves, A. Vassalo, A. Mamede, C. Makhoul, G. Piga, E. Cunha, M. P. M. Marques, L. A. E. Batista de Carvalho, Crystal clear: Vibrational spectroscopy reveals intrabone, intraskeleton, and interskeleton variation in human bones. *Am. J. Phys. Anthropol.* **166**, 296–312 (2018).
- A. M. P. Mamede, D. Gonçalves, M. P. M. Marques, L. A. E. Batista de Carvalho, Burned bones tell their own stories: A review of methodological approaches to assess heat-induced diagenesis. *Appl. Spectrosc. Rev.* **53**, 603–635 (2017).
- M. P. M. Marques, A. P. Mamede, A. R. Vassalo, C. Makhoul, E. Cunha, D. Gonçalves, S. F. Parker, L. A. E. Batista de Carvalho, Heat-induced bone diagenesis probed by vibrational spectroscopy. *Sci. Rep.* **8**, 15935 (2018).
- A. P. Mamede, A. R. Vassalo, G. Piga, E. Cunha, S. F. Parker, M. P. M. Marques, L. A. E. Batista de Carvalho, D. Gonçalves, Potential of bioapatite hydroxyls for research on archeological burned bone. *Anal. Chem.* **90**, 11556–11563 (2018).
- F. Peters, K. Schwarz, M. Eppe, The structure of bone studied with synchrotron x-ray diffraction, x-ray absorption spectroscopy and thermal analysis. *Thermochim. Acta* **361**, 131–138 (2000).
- M. G. Taylor, S. F. Parker, K. Simkiss, P. C. H. Mitchell, Bone mineral: Evidence for hydroxy groups by inelastic neutron scattering. *Phys. Chem. Chem. Phys.* **3**, 1514–1517 (2001).
- G. Cho, Y. Wu, J. L. Ackerman, Detection of hydroxyl ions in bone mineral by solid-state NMR spectroscopy. *Science* **300**, 1123–1127 (2003).
- T. J. U. Thompson, Recent advances in the study of burned bone and their implications for forensic anthropology. *Forensic Sci. Int.* **146**, S203–S205 (2004).
- C. Snoeck, J. A. Lee-Thorp, R. J. Schulting, From bone to ash: Compositional and structural changes in burned modern and archaeological bone. *Palaeogeogr. Palaeoclimatol. Palaeoecol.* **416**, 55–68 (2014).
- P. C. H. Mitchell, S. F. Parker, A. J. Ramirez-Cuesta, J. Tomkinson, *Vibrational Spectroscopy with Neutrons* (Series on Neutron Techniques and Applications 3, World Scientific Press, 2005).
- L. Sarti, Grotta dello Scoglietto (Alberese, Grosseto), in *Predicting Prehistory. Millenni. Studi di Archeologia Preistorica*, G. Pizziolo Eds. (Museo Fiorentino di Preistoria “Paolo Graziosi”, 2015), pp. 157–165.
- V. Leonini, L. Sarti, N. Volante, *Recenti indagini archeologiche nel Parco Naturale della Maremma: la Buca di Spaccasasso e la Grotta dello Scoglietto* (Notiziario SBAT, 1/2005, 2006), pp. 326–328.
- L. Sarti, *Grotta dello Scoglietto (Alberese, Grosseto): Aggiornamento sulle nuove ricerche* (Atti PPE, 2014), vol. 11, pp. 615–624.
- F. R. Stasolla, Leopoli-Cencelle: Il quartiere sud-orientale (Spoleto: Fondazione Centro Italiano di Studi sull’Alto Medioevo, 2012).
- L. Ermini Pani, Il progetto Leopoli – Cencelle, in *Forme e vita di una città medievale Leopoli – Cencelle*. L. Ermini Pani, M. C. Somma, F. R. Stasolla, Eds. (Spoleto: Fondazione Centro Italiano di Studi sull’Alto Medioevo, 2014), pp. 1–13.
- L. Pani Ermini, Leopoli-Cencelle, in *Treccani Encyclopedia* (Treccani, 2004).
- M. F. Rolfo, K. F. Achino, I. Fusco, L. Salari, L. Silvestri, Reassessing human occupation patterns in the inner central Apennines in prehistory: The case-study of Grotta Mora Cavorso. *J. Archaeol. Sci. Rep.* **7**, 358–367 (2016).
- G. Scorrano, M. Baldoni, M. Brilli, M. F. Rolfo, G. Fornaciari, O. Rickards, C. Martínez-Labarga, Effect of Neolithic transition on an Italian community: Mora Cavorso (Jenne, Rome). *Archeol. Anthropol. Sci.* **11**, 1443–1459 (2019).
- T. J. U. Thompson, M. Islam, M. Bonniere, A new statistical approach for determining the crystallinity of heat-altered bone mineral from FTIR spectra. *J. Archaeol. Sci.* **40**, 416–422 (2013).
- T. J. U. Thompson, M. Gauthier, M. Islam, The application of a new method of Fourier transform infrared spectroscopy to the analysis of burned bone. *J. Archaeol. Sci.* **36**, 910–914 (2009).
- C. Roberts, Human remains in archaeology, in *Practical Handbooks in Archaeology* (Council for British Archaeology, 2009), vol. 19.
- H. G. M. Edwards, S. E. J. Villar, J. Parnell, C. S. Cockell, P. Lee, Raman spectroscopic analysis of cyanobacterial gypsum halotrophs and relevance for sulfate deposits on Mars. *Analyst* **130**, 917–923 (2005).
- Y. Yue, Y. Bai, P. A. M. Basheer, J. J. Boland, J. J. Wang, Monitoring the cementitious materials subjected to sulfate attack with optical fiber excitation Raman spectroscopy. *Opt. Eng.* **52**, 104107 (2013).
- P. Falorni, Carta Geografica D’Italia 1:50.000 – Catalogo delle Formazioni, pp. 194–197; http://193.206.192.231/suolo/Accordo-carg/pdf_pub/7071.pdf.
- L. Carnignani, F. A. Decandia, L. Fantozzi, A. Lazzarotto, D. Liotta, M. Meccheri, Tertiary extensional tectonics in Tuscany (Northern Apennines, Italy). *Tectonophysics* **238**, 295–315 (1994).
- C. H. Bachman, E. H. Ellis, Fluorescence of bone. *Nature* **206**, 1328–1331 (1965).
- S. F. Parker, F. Fernandez-Alonso, A. J. Ramirez-Cuesta, J. Tomkinson, S. Rudic, R. S. Pinna, G. Gorini, J. F. Castañon, Recent and future developments on TOSCA at ISIS. *J. Phys. Conf. Ser.* **554**, 012003 (2014).
- S. F. Parker, D. Lennon, P. W. Albers, Vibrational spectroscopy with neutrons: A review of new directions. *Appl. Spectrosc.* **65**, 1325–1341 (2011).
- O. Arnold, J. C. Bilheux, J. M. Borreguero, A. Buts, S. I. Campbell, L. Chapon, M. Doucet, N. Draper, R. Ferraz Leal, M. A. Gigg, V. E. Lynch, A. Markvardsen, D. J. Mikkelsen, R. L. Mikkelsen, R. Miller, K. Palmen, P. Parker, G. Passos, T. G. Perring, P. F. Peterson, S. Ren, M. A. Reuter, A. T. Savici, J. W. Taylor, R. J. Taylor, R. Tolchenov, W. Zhou, J. Zikovsky, Mantid—Data analysis and visualization package for neutron scattering and μ SR experiments. *Nucl. Instrum. Methods Phys. Res. Sect. A* **764**, 156–166 (2014).
- National Institute of Standards and Technology (NIST); <https://www.nist.gov/>.
- Molecular Physical-Chemistry, R&D Unit – University of Coimbra (QFM-UC); www.ci.uc.pt/qfm/.

Acknowledgments: We thank the STFC Rutherford Appleton Laboratory for access to neutron beam facilities [RB’s 1620027 (doi:10.5286/ISIS.E.83550749) and 1810010 (doi:10.5286/ISIS.E.92918618)]. **Funding:** This work was funded by the Portuguese Foundation for Science and Technology (UID/MULTI/00070/2019) and the CNR (Italy) within the CNR-STFC Agreement 2014–2020 (N. 3420) concerning collaboration in scientific research at the ISIS Spallation Neutron Source. **Author contributions:** G.F.: measurement of the INS data, writing of the manuscript, and preparation of figures and tables; C.A.: planning of experimental measurements and contribution to manuscript preparation; M.B.: contribution to manuscript preparation; V.C.: responsible for the artifacts from the Guidonia-Montecelio site and contribution to manuscript preparation; C.M.-L.: contribution to manuscript preparation; F.M.: responsible for the Scoglietto cave samples and contribution to manuscript preparation; O.R.: contribution to manuscript preparation; M.F.R.: responsible for the Mora-Cavorso cave samples and contribution to manuscript preparation; L.S.: responsible for the Scoglietto cave samples and contribution to manuscript preparation; N.V.: responsible for the Scoglietto cave samples and contribution to manuscript preparation; R.S.: contribution to manuscript preparation; F.R.S.: responsible for the Leopoli-Cencelle samples and contribution to manuscript preparation; S.F.P.: measurement and interpretation of the INS data; A.R.V.: measurement of FTIR and INS and preparation of figures; A.P.M.: measurement of FTIR and Raman data and preparation of figures; L.A.E.B.d.C.: measurement of the INS data and interpretation of the vibrational results (INS, FTIR, and Raman); and M.P.M.M.: measurement of the INS data, interpretation of the vibrational results (INS, FTIR, and Raman), and writing of the manuscript. **Competing interests:** The authors declare that they have no competing interests. **Data and materials availability:** All data needed to evaluate the conclusions in the paper are present in the paper and/or the Supplementary Materials. Additional data related to this paper may be requested from the authors.

Submitted 20 November 2018

Accepted 17 May 2019

Published 28 June 2019

10.1126/sciadv.aaw1292

Citation: G. Festa, C. Andreani, M. Baldoni, V. Cipollari, C. Martínez-Labarga, F. Martini, O. Rickards, M. F. Rolfo, L. Sarti, N. Volante, R. Senesi, F. R. Stasolla, S. F. Parker, A. R. Vassalo, A. P. Mamede, L. A. E. Batista de Carvalho, M. P. M. Marques, First analysis of ancient burned human skeletal remains probed by neutron and optical vibrational spectroscopy. *Sci. Adv.* **5**, eaaw1292 (2019).

First analysis of ancient burned human skeletal remains probed by neutron and optical vibrational spectroscopy

G. Festa, C. Andreani, M. Baldoni, V. Cipollari, C. Martnez-Labarga, F. Martini, O. Rickards, M. F. Rolfo, L. Sarti, N. Volante, R. Senesi, F. R. Stasolla, S. F. Parker, A. R. Vassalo, A. P. Mamede, L. A. E. Batista de Carvalho, and M. P. M. Marques

Sci. Adv., **5** (6), eaaw1292.
DOI: 10.1126/sciadv.aaw1292

View the article online

<https://www.science.org/doi/10.1126/sciadv.aaw1292>

Permissions

<https://www.science.org/help/reprints-and-permissions>

Use of this article is subject to the [Terms of service](#)

Science Advances (ISSN 2375-2548) is published by the American Association for the Advancement of Science. 1200 New York Avenue NW, Washington, DC 20005. The title *Science Advances* is a registered trademark of AAAS.

Copyright © 2019 The Authors, some rights reserved; exclusive licensee American Association for the Advancement of Science. No claim to original U.S. Government Works. Distributed under a Creative Commons Attribution NonCommercial License 4.0 (CC BY-NC).